

Experimental and Kinetic Modelling Study of the Impact of NO and NO₂ on the Oxidation of a Primary Reference Fuels Mixture

G. Dayma^{1*}, P. Dagaut²

¹ Université Pierre et Marie Curie (Paris 6)
Institut Jean le Rond d'Alembert, 2 place de la gare de ceinture
78210 Saint Cyr l'Ecole, France

² CNRS, ICARE, 1C avenue de la recherche scientifique
45071 Orléans cedex 2, France

Abstract

New experimental results were obtained for the oxidation of a mixture of 85% of iso-octane and 15% of n-heptane in presence and absence of NO or NO₂ in a fused silica jet-stirred reactor operating at 10 atm, lean conditions and over the temperature range 550-1000 K. Concentration profiles of reactants, intermediates and final products were measured and used to validate a detailed kinetic mechanism. The increased production of OH resulting from the oxidation of NO by HO₂ promotes the oxidation of the fuel in the negative temperature coefficient region but can also inhibit the cool flame region with an increasing NO_x concentration or equivalence ratio.

Introduction

The kinetics of interactions between nitric oxides (NO or NO₂) and fuels have been studied previously, showing that the ignition of simple fuels is promoted by traces of NO [1-7]. This promoting effect is important in several practical systems among which: (i) the NO-NO₂ conversion by hydrocarbons in recent NO_x-reduction strategies, (ii) the modeling of combustion with exhaust-gas recirculation (EGR) such as in Diesel and HCCI (Homogeneous Charge Compression Ignition) engines [8] and mild combustion. Actually, EGR reduces the ignition delays in the engine by a NO_x-promoted oxidation of the fuel and since the firing of HCCI engines is controlled by the fuel ignition kinetics, it is important to take into account this NO_x-hydrocarbon chemistry. Previously, the interactions between iso-octane and NO and n-heptane and NO were only studied for stoichiometric mixtures [9] which is not relevant to HCCI combustion. A more recent study dealing with the oxidation of iso-octane, n-heptane and toluene mixtures sensitized by NO [10] has pointed out the complex impact of NO on surrogate fuels. Therefore, a series of JSR experiments was performed to evaluate the kinetics of the sensitized oxidation of PRF85 by NO and by NO₂ under high pressure and fuel-lean conditions. These new data were used to validate a detailed kinetic reaction mechanism and delineate the important reactions of this system.

Experimental

New experimental results were obtained for the oxidation of a mixture of primary reference fuels sensitized by NO or NO₂. A spherical fused silica jet-stirred reactor (JSR) was used. It was located inside a regulated electrical oven of ~1.5 kW, surrounded by insulating material and a pressure-resistant jacket allowing operation at 10 atm. PRF85 is a mixture of 85% of iso-octane (99.9% pure) and 15% of n-heptane (99.9% pure). This mixture was pumped using a micro piston HPLC pump and sent to an atomizer-vaporizer

assembly maintained at 403 K. A flow of nitrogen (100 L h⁻¹) was used for the atomization. All gases flow rates were measured by thermal mass-flow controllers. NO (>99.995% pure) and oxygen (99.995% pure) were diluted by a flow of nitrogen (<50 ppm of O₂; <100 ppm of Ar; 5 ppm of H₂) and flowed separately up to the mixing point at the entrance of the injectors after preheating. Residence time distribution studies showed that the reactor operates under macro-mixing conditions. A good thermal homogeneity was recorded along the vertical axis of the reactor by a thermocouple (Pt/Pt-Rh 10%) of 0.1 mm diameter located inside a thin-wall fused silica tube to prevent catalytic reactions on the metallic wires. Typical temperature gradients < 2 K.cm⁻¹ were measured. Since we operated under high degree of dilution, the temperature rise due to the reaction was generally < 30 K. Low pressure samples of the reacting mixtures were taken by sonic probe sampling and collected in 1 liter Pyrex bulbs at c.a. 40 mbar for immediate gas-chromatography (GC) analysis.

Two gas chromatographs, equipped with capillary columns (Poraplot U and Plot Al₂O₃/KCl), thermal conductivity detector (TCD) and flame ionization detector (FID) were used for stable species mole fractions measurements. Compounds identification was made through GC/MS analysis of the samples. A quadrupole MS detector operating in electron impact ionization mode (70 eV, GC/MS Varian 1200) was used. Helium was used as a carrier gas. On-line Fourier transform infrared (FTIR) analysis of the reacting gases were also performed by connecting the sampling probe to a temperature controlled (413 K) gas cell (10 m optical path length) via a Teflon heated line (403 K). The sample pressure in the cell was 200 mbar. This analytical equipment allowed the measurements of iso-octane, n-heptane, 2,4,4-trimethylpent-2-ene, 2,4,4-trimethylpent-1-ene, 2,4-dimethylpent-1-ene, 2,4-dimethylpent-2-ene, 4,4-dimethylpent-1-ene, 4,4-dimethylpent-2-ene, heptenes, hex-1-ene, pent-1-ene,

* Corresponding author: guillaume.dayma@upmc.fr

iso-butene, but-1-ene, propene, ethylene, CH₄, CH₂O, CO, CO₂, H₂O, NO, NO₂ and HCN. As previously [3], very good agreement between the GC and FTIR analysis was found for the compounds measured by both techniques (CO, CO₂ and C₂H₄). Carbon balance was checked for every sample and found good (100+/-5%). The mole fractions of NO and NO₂ were determined to within +/- 5-25 ppm, depending on the initial concentrations.

Kinetic modelling

For the chemical kinetic modelling, the PSR computer code [11] was used. The proposed kinetic reaction mechanism (1085 species and 4405 reversible reactions) derives from the detailed kinetic mechanism proposed by [12] for primary reference fuels and an updated version of the kinetic scheme developed for the mutual oxidation of NO and hydrogen, methane, methanol, ethane, ethylene and a natural gas blend [1, 2, 4, 5]. Alkoxy β -scissions rate constants used in [9] were updated following recent recommendations made by [13]. New reactions were also added for alkoxy at low temperature. The NO_x sub-scheme was partially updated following recently proposed mechanisms [14, 15], and specific reactions of alkylperoxides and NO were added with rate constants from [16, 17]. The rate constants for the reverse reactions were computed from the forward rate constants and the appropriate equilibrium constants calculated using thermochemical data. The full mechanism, including thermochemical data, is available from the authors (guillaume.dayma@upmc.fr).

Results and discussion

A large set of experimental results was obtained for the oxidation of PRF85, PRF85/NO and PRF85/NO₂ mixtures, over the temperature range 550-1000 K, for equivalence ratios of 0.2, 0.5, and 0.7 at 10 atm. The residence time of 0.5 s was kept constant during the experiments. First, we have investigated the evolution of the mole fractions against the temperature: the initial concentration of PRF85 was 1000 ppm, that of NO was either 0, 50, or 200 ppm and that of NO₂ was either 0 or 50 ppm. Second, the temperature was kept constant at 660 K or 750 K and the initial mole fraction of NO was varied from 0 to 1000 ppm.

Figure 1 depicts the influence of an increased initial concentration of NO from 0 to 200 ppm on the evolution of the mole fraction of iso-octane for an equivalence ratio of 0.2. The sensitized oxidation of PRF85 under these conditions showed the three regimes of oxidation well-known for large hydrocarbons, namely cool flame, negative temperature coefficient (NTC), and high temperature oxidation. When the initial concentration of NO increases, the low temperature (550-650 K) reactivity starts at a higher temperature: the effect of an addition of 50 ppm can not be clearly seen experimentally whereas the addition of 200 ppm of NO shifts the starting temperature of the cool flame of c.a. 30 K towards the highest temperatures. Another effect

of the addition of NO can be seen in the intermediate temperature region (650-850 K). The NTC behaviour is less and less pronounced when the initial concentration of NO is increased: when introducing 200 ppm of NO, the NTC is so attenuated that we can not talk anymore about a decrease of the conversion while the temperature increases, but just a plateau in the consumption of iso-octane that could be also observed on n-heptane conversion but not shown here for clarity matter. Over the high temperature oxidation range (> 750 K), the increased initial concentration of NO seems to promote the fuel consumption: the conversion starts c.a. 25 K lower with 200 ppm of NO added.

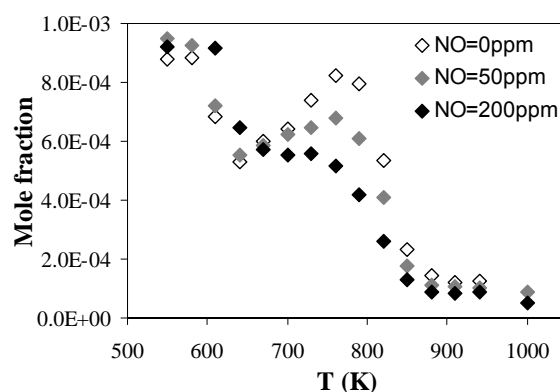


Figure 1: Evolution of the mole fraction of iso-octane versus temperature at 10 atm, $\tau = 0.5$ s and $\phi = 0.2$ for three different initial mole fractions of NO.

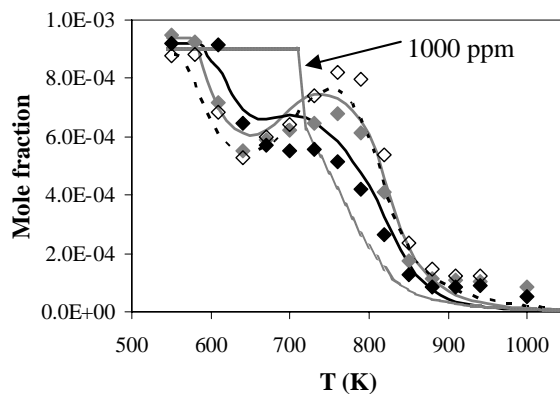


Figure 2: Comparison between experimental (symbols) and numerical (lines) mole fractions of iso-octane versus temperature at 10 atm, $\tau = 0.5$ s and $\phi = 0.2$ for initial mole fractions of NO of 0 ppm (open diamonds, dashed line), 50 ppm (grey diamonds, grey line) and 200 ppm (black diamonds, black line) and simulated profile for 1000 ppm (shadowed line).

The developed detailed kinetic mechanism was used to investigate the effect of higher initial concentrations of NO. Figure 2 presents a comparison between our experimental results obtained with 0, 50, and 200 ppm of NO and the numerical results obtained in the same conditions thanks to our kinetic scheme. Also reported on figure 2, are the results of the calculations with 1000

ppm of NO added. It appears that increasing the initial concentration of NO inhibits the fuel conversion at low temperature (~ 600 K), increases the reactivity in the NTC region (~ 650 - 750 K) and promotes the fuel conversion at higher temperature (~ 800 K). For an initial concentration of NO of 1000 ppm, our mechanism shows that the three regimes of oxidation has disappeared to give only one zone of consumption against the temperature, starting at higher temperature than without NO but consuming all the fuel at lower temperature. Under these conditions, the low temperature reactivity seems to disappear for an initial concentration of NO around 500 ppm which is not well reproduced by the model. Our model still predicts a cool flame for 500 ppm and the transition apparently occurs around 700 ppm of NO.

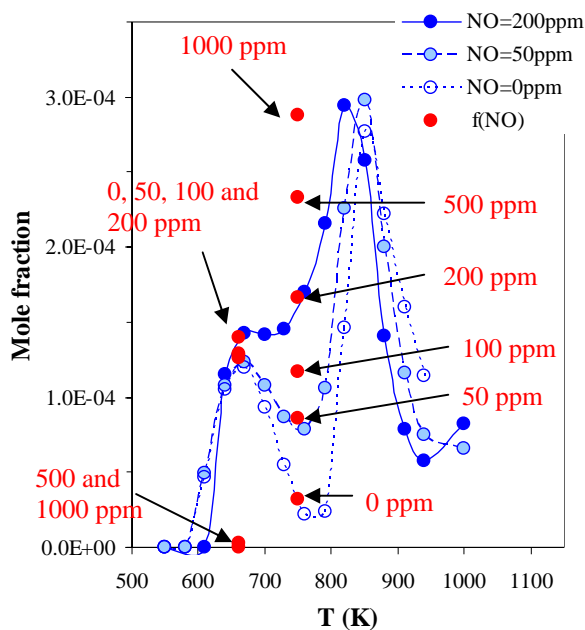


Figure 3: Evolution of the experimental mole fraction of formaldehyde versus temperature at 10 atm, $\tau = 0.5$ s and $\phi = 0.2$ for three different initial mole fractions of NO and for 0, 50, 100, 200, 500, and 1000 ppm of initial NO at 660 K and 750 K (in red). Lines represents tendency curves.

In order to validate these calculations for high initial concentrations of NO, two experiments at fixed temperatures with various initial concentrations of NO were performed. These two temperatures are 660 K, where the maximum of the cool flame without NO was observed and 750 K, where the maximum of the negative temperature coefficient was observed. The experimental results are presented in Figure 3 for formaldehyde (CH₂O) which is a good tracer of the reactivity all over the temperature range. On this figure is plotted the evolution of the mole fractions of formaldehyde against the temperature for 0, 50, and 200 ppm of NO added and the formaldehyde mole fractions at 660 K and 750 K for 0, 50, 100, 200, 500 and 1000 ppm of initial NO. Over the low temperature region (~ 660 K), up to 200 ppm of NO, increasing the initial

concentration of NO does not seem to have any impact on the cool flame intensity: i.e. the addition of NO does not change the maximum mole fraction of CH₂O in the cool flame. In the negative temperature coefficient region (~ 750 K), the mole fraction of formaldehyde increases continuously when the initial concentration of NO increases. At this temperature, with 1000 ppm of NO, the mole fraction of CH₂O has reached its maximum value observed in the high temperature region. Therefore figure 3 confirms the disappearance of the cool flame regime for an initial mole fraction of NO between 200 ppm and 500 ppm.

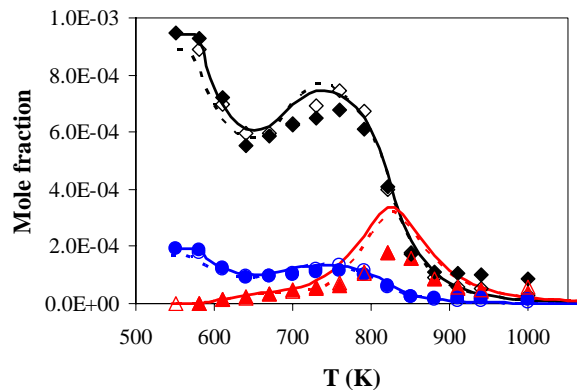


Figure 4: Evolution of the mole fractions of iso-octane (black), n-heptane (blue) and iso-butene (red) against temperature, at 10 atm, $\tau = 0.5$ s and $\phi = 0.2$. Open symbols and dashed lines for NO₂ = 50 ppm and filled symbols and continuous lines for NO = 50 ppm. Lines represent numerical results.

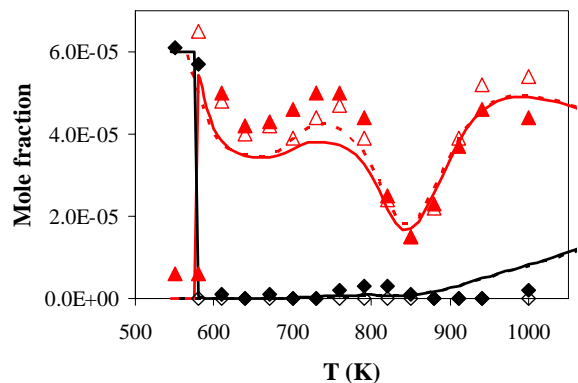


Figure 5: Evolution of the mole fractions of NO (black) and NO₂ (red) against temperature at 10 atm, $\tau = 0.5$ s and $\phi = 0.2$. Open symbols and dashed lines for initial NO₂ = 50 ppm and filled symbols and continuous lines for initial NO = 50 ppm. Lines represent numerical results.

The nature of the introduced nitrogenous species was also investigated. Figures 4 and 5 present respectively the evolution of the mole fractions of iso-octane, n-heptane and iso-butene, and NO and NO₂, at 10 atm, $\tau = 0.5$ s and $\phi = 0.2$. Experimentally, as well as numerically, no difference can be noticed between the

profiles of iso-octane in both conditions. Figure 5 can give an explanation to this phenomenon: when NO is added, as soon as the fuel oxidation starts, NO is quickly converted into NO₂ and then, only NO₂ remains all over the temperature range. Thus, in these conditions, as NO₂ is instantaneously formed at every temperature, it is the chemistry of NO₂ which drives the reactivity. Another interesting point arising figure 5 is the strong depletion in NO₂ mole fraction which is not compensated by NO formation. According to our mechanism, NO₂ is consumed at around 850 K to form nitromethane, CH₃NO₂. This compound was identified by FTIR analysis but not quantified due to high levels of water which absorbs in the same spectrum region. Reactions for the consumption of nitromethane from [18, 19, 20] were added into our mechanism.

Figure 6 proposes the evolution of the mole fractions of NO, NO₂, CH₃NO₂, HONO, and HONO₂ to rationalize the shape of NO₂ profile at 10 atm, $\tau = 0.5$ s, $\phi = 0.2$, and 50 ppm of initial NO. As noted before, NO is quickly converted into NO₂ at every temperatures, then, between 580 and 700 K, HONO₂ is formed by addition of NO₂ with OH radicals. HONO is also formed, all over the temperature range, by addition of NO with OH. These last two reactions are favored by the high pressure via a third body action. Nitromethane is significantly formed above 600 K with a local maximum in the cool flame region and becomes the major nitrogenous species at 850 K. CH₃NO₂ comes from the recombination of CH₃ and NO₂ with the help of a third body. As stated by [14], this reaction is also favored by the high pressure in our experiments. The total fixed nitrogen (except N₂) which corresponds to sum of the considered nitrogenous species is also plotted on Figure 6: this indicates that no other nitrogen containing species are significantly produced in the temperature range studied. Nitrous acid (HONO) and HONO₂ were not experimentally detected because their response is very low in the IR.

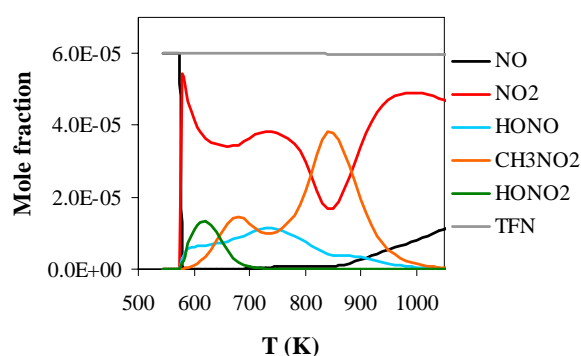


Figure 6: Computed mole fractions of NO (black), NO₂ (red), HONO (blue), CH₃NO₂ (orange) and HONO₂ (green) against the temperature at 10 atm, $\tau = 0.5$ s, $\phi = 0.2$ and initial NO = 50 ppm according to our chemical kinetic mechanism (total fixed nitrogen except N₂ is plotted in grey).

Finally, the effect of the equivalence ratio was also studied. Figure 7 illustrates the impact of the addition of 200 ppm of NO on iso-octane oxidation for three different equivalence ratios (0.2, 0.5, and 0.7). The results indicate that the effect on the NTC of an addition of NO is similar whatever the equivalence ratio is: the negative temperature coefficient is erased by the presence of 200 ppm of NO. In the same experimental conditions, Figure 8 presents the evolution of the mole fractions of NO and NO₂ against the temperature for equivalence ratios of 0.2 and 0.7. It appears that the temperature at which the conversion of NO into NO₂ starts is shifted towards higher values when the equivalence ratio increases. This trend is quite well captured by the model. Nevertheless, in the low temperature region for an equivalence ratio of 0.7, NO is remaining and this is not predicted by our kinetic scheme. For an equivalence ratio of 0.2, the mole fraction of NO between 650 and 850 K is less than 1 ppm whereas for $\phi = 0.7$, it reaches 83 ppm at 730 K. This behavior is also observed for the equivalence ratio of 0.5. This phenomenon was also noted by [8] but only with iso-octane ($p = 10$ atm, $\tau = 1$ s, $\phi = 1$ and $X_{\text{iso-octane}} = 1250$ ppm) and not with pure n-heptane, whatever the initial concentration of NO was. Two explanations of this behavior can be offered. First, since NO reacts mainly with HO₂, the concentration of hydroperoxyl radicals may be not sufficient to convert all the available NO. This implies that the HO₂ formation and consumption is not well predicted by the PRF model, and more precisely, in the iso-octane sub-scheme. This is usually without consequences since HO₂ is not an important radical as far as the reactivity of alkanes is concerned. Second, since NO₂ is over predicted by our model, we could miss a partner for the reduction of NO₂ into NO in the low temperature region or, it could be helpful to consider the formation of alkylnitrates as suggested by [10, 21]. This means that the reactions between nitrogenous species and hydrocarbons related compounds must be investigated further, particularly over the low temperature region.

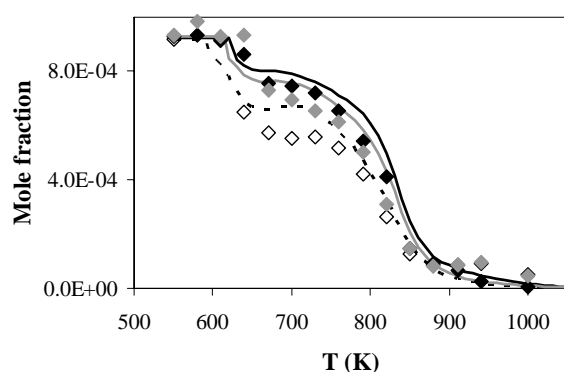


Figure 7: Evolution of the mole fraction of iso-octane as a function of temperature at 10 atm, $\tau = 0.5$ s and for equivalence ratios 0.2 (open diamonds, dashed line), 0.5 (grey diamonds, grey line) and 0.7 (black diamonds, black line). The data (symbols) are compared to the computations (lines).

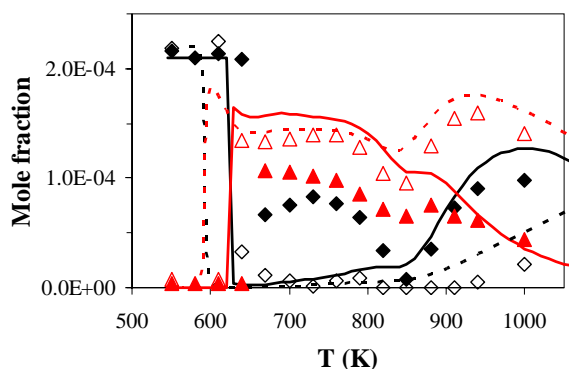


Figure 8: Evolution of the mole fractions of NO (black) and NO₂ (red) as a function of temperature at 10 atm, $\tau = 0.5$ s and for equivalence ratios of 0.2 (open symbols, dashed lines), and 0.7 (filled symbols, lines). The data (symbols) are compared to the computations (lines).

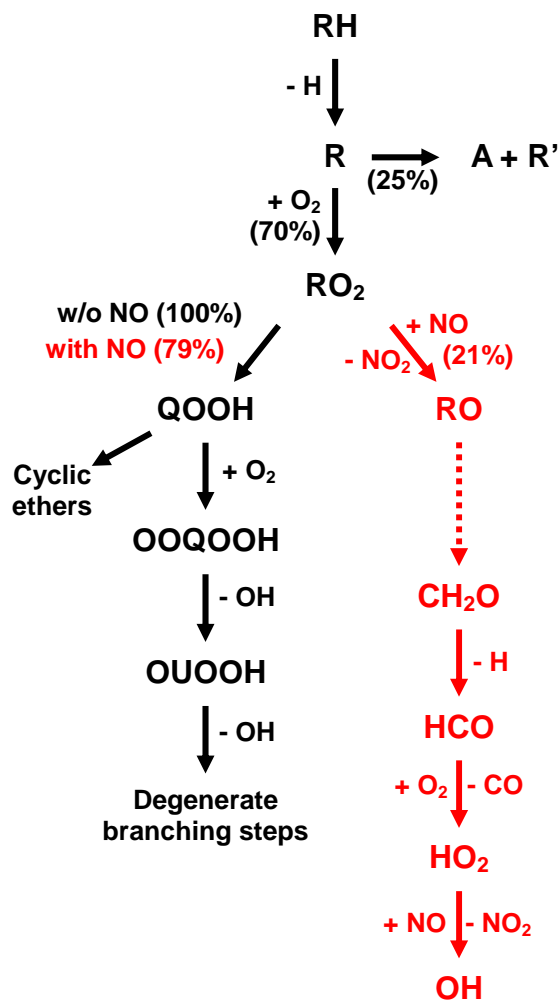


Figure 9: Main pathways for the consumption of iso-octane at 10 atm, $\tau = 0.5$ s, $\phi = 0.2$, and $T = 730$ K. Routes and annotations without NO_x are in black and alternative routes with 200 ppm of initial NO in red. Numbers in brackets represent the flow rates in the studied conditions.

In order to explain the particular phenomenon of the negative temperature coefficient and cool flame disappearance, two reaction rates analyses were performed at 730 K, $\phi = 0.2$ and an initial concentration of NO of either 0 or 200 ppm. These analyses are summarized in Figure 9. At 730 K, iso-octane mainly reacts by H-abstraction with OH with or without NO_x. For all the stable compounds, the difference observed with and without NO_x concerns H-abstractions: when NO_x are added, H-abstractions in this temperature range are exclusively with OH. Hydroxyl radicals are the only reactants because HO₂ is mostly consumed by NO+HO₂ giving NO₂+OH. This does not make a huge difference since H-abstractions with HO₂ represent only few percents of the total consumption of each compound. The main difference comes from the amount of reactants consumed: at this temperature, the rate of consumption of iso-octane is 4.69×10^{-8} mol cm⁻³ s⁻¹ without NO_x and 8.95×10^{-8} mol cm⁻³ s⁻¹ with 200 ppm of NO due to the increased concentration of OH. In these conditions, the flow of β -scissions increases when NO is added even though the relative flow remains constant (~25%). A and R' are an alkene and a radical that has no other route than add with O₂ at this temperature. The same apply to iso-octyl radicals. Once more, at this stage, the routes of consumption of the fuel are the same with or without NO_x. The difference comes from the amount of treated species. Without NO, peroxy compounds (RO₂) all isomerize into alkylhydroperoxy compounds (QOOH). With the addition of 200 ppm of NO, 21% of the peroxy compounds react with NO to give an alkoxy and NO₂. So, the addition of NO promotes the formation of alkoxy compounds. These alkoxy, most of them primary due to iso-octane, are consumed to give formaldehyde. Formaldehyde then follows the usual route through formyl radicals to form CO and HO₂. Without NO, this final step is almost a termination step since H₂O₂, mostly formed by the recombination of HO₂ with itself, does not react to form two OH at this temperature. With NO, HO₂ is readily converted into OH which constitutes the key step to explain the disappearance of the negative temperature coefficient in presence of NO: thanks to NO_x, OH radicals are formed at temperatures where there is usually much less OH, allowing the fuel conversion to start at lower temperature.

The formation of alkoxy radicals at low temperature is also responsible for the disappearance of the cool flame when the initial concentration of NO increases. Removing a part of the peroxy radicals, NO reduces the opportunity for these compounds to yield two OH radicals via the formation of degenerated branching agents. Moreover, high NO concentration promotes the formation of HONO, which is also more stable at high pressure. Hence, NO is less regenerated by the reduction of NO₂, and HO₂ is less converted into OH and the reactivity decreases up to disappearance.

Conclusion

New data were obtained for the oxidation of a mixture of primary reference fuels (PRF85) in absence and presence of NO or NO₂. A detailed chemical kinetic mechanism was proposed for modelling these experimental results. A good agreement between the data and the modelling was obtained for all the experimental conditions for the hydrocarbons. Nitrogenous compounds are also well predicted except at low temperature, for equivalence ratios 0.5 and 0.7 where NO seem to remain. According to the model, the mutual sensitization of the oxidation of PRF85 and NO proceeds through the NO to NO₂ conversion by HO₂. This additional production of OH resulting from the oxidation of NO by HO₂ promotes the oxidation of the fuel allowing the conversion to start at lower temperature: in the negative temperature coefficient region, the addition of NO allows the production of OH from HO₂, increasing the reactivity. However, when the concentration of NO increases, the starting temperature of the cool flame also increases until the cool flame disappears. These phenomena are related to formation of alkoxy radicals via: ROO+NO→RO+NO₂ and the stabilization of HONO over high pressure that removes NO from the system.

References

- [1] P. Dagaut, O. Mathieu, A. Nicolle, G. Dayma, *Combust. Sci. Technol.* 177 (2005) 1767.
- [2] G. Dayma, P. Dagaut, *Proc. Combust. Inst.* 31 (2007) 411.
- [3] R. Siviramanakrishnan, K. Brezinsky, G. Dayma, P. Dagaut *Phys. Chem. Chem. Phys.* 9 (2007) 4230.
- [4] G. Dayma, P. Dagaut, *Combust. Sci. Technol.* 178 (2006) 1999.
- [5] P. Dagaut, G. Dayma, *J. Phys. Chem. A* 110 (2006) 6608.
- [6] T. Faravelli, A. Frassoldati, E. Ranzi, *Combust. Flame* 132 (2003) 188.
- [7] P.A. Glaude, N. Marinov, Y. Koshiishi, N. Matsunaga, M. Hori, *Energy and Fuels* 19 (2005) 1839.
- [8] G. Moréac, P. Dagaut, J.F. Roesler, M. Cathonnet, *Combust. Flame* 145 (2006) 512.
- [9] A. Dubreuil, F. Foucher, C. Mounaim-Rousselle, G. Dayma, P. Dagaut, *Proc. Combust. Inst.* 31 (2007) 2879.
- [10] J.M. Andelohr, R. Bounaceur, A. Pires Da Cruz, F. Battin-Leclerc, *Combust. Flame* 156 (2009) 505.
- [11] P. Glarborg, R.J. Kee, J.F. Grcar, J.A. Miller, *PSR : A FORTRAN program for modeling well-stirred reactors*, Report N°. SAND86-8209, Sandia National Laboratories, 1986.
- [12] H.J. Curran, W.J. Pitz, C.K. Westbrook, C.V. Callahan, F.L. Dryer, *Proc. Combust. Inst.* 27 (1998) 379.
- [13] H.J. Curran, *Int. J. Chem. Kinet.* 38 (2006) 250.
- [14] C.L. Rasmussen, A.E. Rasmussen, P. Glarborg, *Combust. Flame* 154 (2008) 529.
- [15] C.L. Rasmussen, J. Hansen, P. Marshall, P. Glarborg, *Int. J. Chem. Kinet.* 40 (2008) 454.
- [16] J. Eberhard, J.H. Howard, *Int. J. Chem. Kinet.* 28 (1996) 731.
- [17] J. Eberhard, P.W. Villalta, C.J. Howard, *J. Phys. Chem.* 100 (1996) 993.
- [18] P. Glarborg, A.B. Bendtsen, J.A. Miller, *Int. J. Chem. Kinet.* 31 (1999) 591.
- [19] J.C. Tricot, A. Perche, M. Lucquin, *Combust. Flame* 40 (1981) 269.
- [20] Y. Zhang, S.H. Bauer, *J. Phys. Chem. B* 101 (1997) 8717.
- [21] W. Chan, S.M. Heck, H.O. Pritchard, *Phys. Chem. Chem. Phys.* 3 (2001) 56.